Rapid phase change of lipid microdomains in giant vesicles induced by conversion of sphingomyelin to ceramide

ARTICLE *in* BIOCHIMICA ET BIOPHYSICA ACTA · MARCH 2006

Impact Factor: 4.66 · DOI: 10.1016/j.bbamem.2006.02.026 · Source: PubMed

4 AUTHORS, INCLUDING:

Yukinori Taniguchi

Japan Advanced Institute of Science and T…

18 PUBLICATIONS **159** CITATIONS

Available online at www.sciencedirect.com
SCIENCE DIRECT
Biochimica et Biophysica Acta 1758 (2006) 145 – 153
BIOCHIMICA ET BIOPHYSICA ACTA
BBA
http://www.elsevier.com/locate/bba

Rapid phase change of lipid microdomains in giant vesicles induced by conversion of sphingomyelin to ceramide

Yukinori Taniguchi [1], Tetsuhiko Ohba, Hidetake Miyata, Kazuo Ohki *

Department of Physics, Graduate School of Science, Tohoku University, Aza-aoba, Aramaki, Aoba-ku, Sendai 980-8578, Japan

Received 22 June 2005; received in revised form 13 February 2006; accepted 17 February 2006
Available online 3 April 2006

Abstract

To understand the role of sphingomyelinase (SMase) in the function of biological membranes, we have investigated the effect of conversion of sphingomyelin (SM) to ceramide (Cer) on the assembly of domains in giant unilamellar vesicles (GUVs). The GUVs were prepared from mixture of 1,2-dioleoyl-*sn*-glycero-3-phosphocholine (DOPC), *N*-palmitoly-D-*erythro*-sphingosine (C_{16}Cer), *N*-palmitoyl-D-*erythro*-sphingosylphosphorylcholine (C_{16}SM) and cholesterol. The amounts of DOPC, sum of C_{16}Cer and C_{16}SM, and cholesterol were kept constant (the ratio of these four lipids is shown as 1:*X*:1–*X*:1 (molar ratio), i.e., *X* is C_{16}Cer/(C_{16}Cer+C_{16}SM)). Shape and distribution of domains formed in the GUVs were monitored by a fluorescent lipid, Texas Red 1,2-dihexadecanoyl-*sn*-glycero-3-phosphoethanolamine (0.1 mol%). In GUVs containing low C_{16}Cer (*X*=0 and 0.25), round-shaped domains labeled by the fluorescent lipid were present, suggesting coexistence of liquid-ordered and disordered domains. In GUVs containing intermediate Cer concentration (*X*=0.5), the fluorescent domain covered most of GUV surface, which was surrounded by gel-like domains. Differential scanning calorimetry of multilamellar vesicles prepared in the presence of higher Cer concentration ($X \geq 0.5$) suggested existence of a Cer-enriched gel phase. Video microscopy showed that the enzymatic conversion of SM to Cer caused rapid change in the domain structure: several minutes after the SMase addition, the fluorescent region spread over the GUV surface, within which regions with darker contrast existed. Image-based measurement of generalized polarization (GP) of 6-dodecanoyl-2-dimethylaminonaphthalene (Laurdan), which is related to the acyl chain ordering of the lipids, was performed. Before the SMase treatment domains with high (0.65) and low (below 0.4) GP values coexisted, presumably reflecting the liquid-ordered and disordered domains; after the SMase treatment regions with intermediate GP values (0.5) and smaller regions with higher GP values (0.65) were present. Generation of Cer thus caused a phase transition from liquid-ordered and disordered phases to a gel and liquid phase.

Keywords: Sphingomyelinase; Lipid raft; Lipid microdomain; Giant liposome; Generalized polarization imaging

1. Introduction

In the cell, lipid microdomains (rafts), a putative membrane regions enriched with sphingolipids and cholesterol, are believed to provide a platform for signaling molecules [1–3]. A presumed role of the lipid microdomains is to concentrate the molecules involved in the signal transduction, thereby regulating the efficiency of the signal transduction process. However, the entity of lipid microdomains is controversial [4–10].

To study the physicochemical principle of organization of lipid microdomains, giant unilamellar vesicles (GUVs) composed of ternary mixture of cholesterol, saturated and unsaturated phospholipids have been used as a model system that exhibits liquid-ordered and liquid-disordered phase separation [11–16]. In these studies mainly two approaches have been taken. One is to study the effect of depletion or modification of cholesterol with β-cyclodextrin [17] or cholesterol oxidase [13] that have been shown to destroy organization of lipid microdomains in vivo [18–20].

Another is to study the effect of conversion of sphingomyelin (SM) into ceramide (Cer) by sphingomyelinase (SMase). SM is one of the major lipid components of lipid microdomains and Cer is a well-known mediator in the lipid signaling process ([21]

* Corresponding author. Tel.: +81 22 795 6464; fax: +81 22 795 6774.
E-mail address: ohki@bio.phys.tohoku.ac.jp (K. Ohki).
[1] Present address: Department of Bioscience, Graduate School of Science and Technology, Kwanseigakuin University, 2-1 Gakuen, Sanda 669-1337, Japan.

0005-2736/$ - see front matter © 2006 Elsevier B.V. All rights reserved.
doi:10.1016/j.bbamem.2006.02.026

for review). In in vitro studies, the effect of Cer on phase separation in lipid membranes composed of Cer, SM and/or a single kind of phosphatidylcholine have been investigated [22–33]. For example, SMase treatment of GUVs composed of 1-stearoyl-2-oleoyl-*sn*-glycero-3-phosphocholine (SOPC) and SM induces Cer-rich domains and change in the topology of membranes [24]. However, the effect of Cer on the separation of liquid-ordered and liquid-disordered phases remains unknown. Recently, it has been shown that Cer displaces cholesterol from detergent resistant membrane (DRM) fraction prepared from the ternary mixture of DOPC, 1,2-dipalmitoyl-*sn*-glycero-3-phosphocholine (DPPC) and cholesterol [34], and this was attributed to disassembly of liquid-ordered and liquid-disordered domains by Cer. In the cell, production of Cer catalyzed by SMase occurs mainly in the outer leaflet of the plasma membrane because almost all SM molecules reside there [35]. Hence, the dynamic and asymmetric production of Cer in the cell may alter the domain structure of the cell membranes.

In this study, we observed the effect of the enzymatic conversion of SM to Cer on the pre-existing lipid domains on GUVs prepared from the mixture of 1,2-dioleoyl-*sn*-glycero-3-phosphocholine (DOPC)/*N*-palmitoyl-D-*erythro*-sphingosine (C_{16}Cer)/*N*-palmitoyl-D-*erythro*-sphingosylphosphorylcholine (C_{16}SM)/cholesterol. The GUVs were visualized under fluorescence microscope either with a dye-tagged lipid, 1,2-dihexadecanoyl-*sn*-glycero-3-phosphoethanolamine conjugated with Texas Red (TR-DPPE), which is predominantly distributed in liquid-disordered phase [12,14,17], or with an environment-sensitive dye, 6-dodecanoyl-2-dimethylaminonaphthalene (Laurdan) [12,36–38]. Two different types of domains corresponding to high and low ratios of Cer to SM were observed. Furthermore, dynamic change occurred in the structure and morphology of domains that existed at low Cer/SM ratio as a result of enzymatic action of SMase on GUVs.

2. Materials and methods

2.1. Materials

DOPC, C_{16}SM and C_{16}Cer were purchased from Avanti Polar Lipids, Inc. (Alabaster, AL). Cholesterol and trinitrophenylaminolauroylsphingomyelin (TNPAL-SM) were from Sigma-Aldrich Co. (St. Louis, MO). TR-DPPE and Laurdan were from Molecular Probes, Inc. (Eugene, OR). The lipids were used without further purification.

SMase from *Streptomyces* sp. (Sigma-Aldrich Co.) was dissolved in a buffer (10 mM HEPES–NaOH, 0.1 mg/ml BSA, pH 7.4) dialyzed against the same buffer and was checked for the enzymatic activity by using TNPAL-SM [39]. The concentration of SMase ranged from 10 to 20 U/ml, where one unit will hydrolyze 1.0 μmole of TNPAL-SM per min at pH 7.4 at 37 °C.

2.2. Preparation of GUVs and multilamellar vesicles

GUVs were prepared by gentle hydration method [40,41]. A 40-μl mixture of lipids and a dye (7.5 mg/ml in 2:1 (v/v) mixture of chloroform/methanol) in a glass test tube attached to a rotary evaporator was dried at 45 °C to form a thin lipid film on the bottom of the test tube. Then, the tube was placed in vacuo for at least 3 h to remove trace of organic solvents. After 3 ml of "internal buffer" (100 mM sucrose, 10 mM $MgCl_2$, 10 mM HEPES–NaOH, pH 7.4) was added, the tube was incubated at >50 °C overnight to hydrate the lipids. When GUVs were labeled with TR-DPPE or Laurdan, the label was mixed with chloroform–methanol solution of lipids before the drying process. In this paper, we describe the molar ratio of lipids in the mixture containing DOPC, C_{16}Cer, C_{16}SM and cholesterol as follows: 1:*X*:1–*X*:1, where $X = C_{16}Cer/(C_{16}Cer + C_{16}SM)$.

To prepare multilamellar vesicles (MLVs), a mixture of lipids (7.5 mg total lipid/ml in 2:1 (v/v) mixture of chloroform/methanol) in a glass vial was dried under a stream of nitrogen. The vial was placed in vacuo for at least 3 h to remove all traces of the organic solvent. After 1.5 ml of 10 mM HEPES–NaOH (pH 7.4) was added, the solution was mixed vigorously with a vortex mixer and incubated at >90 °C for at least 3 h. Final concentration of lipids in the MLV preparation was 3 mM.

2.3. Observation of GUVs

The GUV suspension prepared as the above method was transferred into an observation chamber containing an "external buffer" (120 mM glucose, 10 mM $MgCl_2$, 10 mM HEPES–NaOH, pH 7.4). The sugar concentration of the external buffer (120 mM) is slightly higher than that of the internal buffer (100 mM) because we expected to avoid osmotic pressure-caused burst of the GUVs. The difference in the sugar species between the external and the internal buffers facilitated sedimentation of GUVs on a cover glass owing to the difference in the specific gravity, and enhanced the contrast of GUVs against the surrounding medium under phase-contrast light microscope (Fig. 1A) [40,42]. The cover glass that formed the bottom of the chamber had been washed and coated either with agarose or with BSA and poly-L-lysine to prevent adhesion of GUVs [41]. GUVs were observed at room temperature (22–25 °C) with an inverted epi-fluorescence microscope (Axiovert S100, Carl Zeiss, Inc., Tokyo) equipped with an objective (×40, NA = 0.75. Plan Neofluar, Carl Zeiss Inc.), and the images of GUVs labeled with TR-DPPE were acquired with an image-intensified charge-coupled device (CCD) camera (C2400-89, Hamamatsu Photonics, Hamamatsu, Japan). The lamellarity of GUV was estimated based on the fluorescence intensity of the membranes of GUVs stained with TR-DPPE [40].

The SMase solution was applied with a micropipette (inner diameter ~10 μm) to the external surface of individual GUVs. As shown in Fig. 1A, the flow of SMase solution was controlled by hydrostatic pressure between the stage and the surface of water in a column connected to the micropipette [40].

2.4. Measurement of generalized polarization

To evaluate the ordering of acyl chains, GUVs were labeled with Laurdan and a parameter called generalized polarization (GP, see below) was measured with a

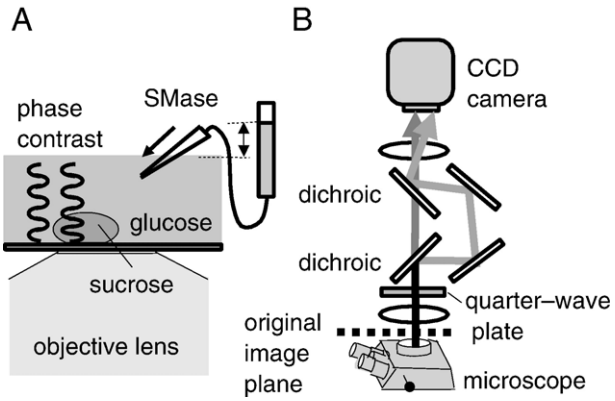

Fig. 1. Schematic representations of (A) observation chamber and (B) dual-color imaging system. (A) GUVs were formed in a solution containing sucrose and placed in a solution containing glucose. The GUVs were settled on a cover glass with enhanced contrast owing to the difference in specific gravity and refractive index between glucose and sucrose. SMase solution was delivered to the target GUV from a micropipette, which was connected to a water column for the control of hydrostatic pressure. (B) In the dual-color imaging apparatus, the fluorescence image was split into two separate images with a dichroic mirror, which reflect the light below 465 nm, and the two images were focused on different regions of the chip of a cooled CCD camera.

home-built microscopic imaging instrument [38]. Laurdan shows the shift in the peak of emission spectrum, which is linearly correlated with the polarity of the solvent [43]. In lipid membranes, this shift occurs with the change in the water content in the vicinity of the dye, and can be related to the ordering of acyl chains [36]. The emission shift is quantified with the GP value, which also provides a method to visualize the lipid domains [12,38,44]. The GP value is defined as

$$\mathrm{GP} = \frac{I_{440^{-g}} I_{490}}{I_{440^{+g}} I_{490}}, \quad (1)$$

where and correspond to the fluorescence intensities at 440 nm and 490 nm, respectively [36,37]. The g factor corrects the wavelength dependence of the sensitivity of detection system, and was obtained under the assumption that the GP value of DPPC MLVs in gel phase, which was measured under fluorescence microscope, was equal to that determined for the same sample in spectro-fluorophotometer (GP=0.6, agreed with the literature values [12,37]).

To achieve the image-based quantification of GP values, the GUV solution was illuminated by the light passed through a 365 nm band-pass filter. The fluorescence was collected with an apochromat objective (×40, NA=0.95 Plan Apochromat, Carl Zeiss, Inc.), passed through a home-built dual-color imaging module (Fig. 1B) [38,45] and acquired with a cooled CCD camera (C4742-95, Hamamatsu Photonics). The dual-color imaging module splits the fluorescence image with a dichroic mirror, which reflects the light below 465 nm, into two separate images and focuses them on different regions of the chip of the CCD camera. To reduce polarization dependence of reflectance of dichroic mirrors, a quarter-wave plate was placed before the dichroic mirror. The acquired images were superimposed at a sub-pixel resolution using affine transformation (i.e., rotation, lateral shift and scaling of two images) after subtraction of background intensity. The parameters used for the transformation were determined from an image of 10 μm-grid acquired in the same manner. GP values of individual pixels were calculated according to the above equation [38,46,47].

2.5. Differential scanning calorimetry of MLVs

Differential scanning calorimetry (DSC) measurements were performed with a differential adiabatic microcalorimeter (DASM-4, Privalov) at a heating rate of 0.5 K/min under 2.0 atm to prevent bubble formation [48]. Repeated scanning except for the first scan showed no change in the shape of thermogram. Total lipid concentration was 3 mM.

2.6. Measurement of activity of SMase in GUVs

The hydrolysis of SM in GUVs was measured by thin-layer chromatography (TLC). A 1 ml of GUV suspension (containing 50 nmol C_{16}SM) was incubated for 10 min at 25 °C in the presence of 0.2 U of SMase solution in 10 μl. Then, 0.5 ml of chloroform/methanol (2:1) was added to the suspension and mixed vigorously. After centrifugation at 1000×g for 5 min, the aqueous phase was completely removed. Then, chloroform was dried to obtain a lipid film, which was resuspended in 5 μl of chloroform/methanol 2:1, applied to TLC plate and was developed in the TLC solvent (1,2-dichloroetane/methanol/water=90:20:0.5 (v/v) [49]). Upon staining lipids with primuline (Nacalai tesque, Inc., Kyoto), three bands corresponding to SM with DOPC, cholesterol and Cer were observed. The images of the bands were video-recorded and the staining intensities of SM with DOPC in the presence and absence of SMase ($I_{sd}^{\pm SMase}$) and those of cholesterol ($I_{chol}^{\pm SMase}$) were quantified with ImageJ program (ver. 1.26). Fraction of hydrolyzed SM was calculated as $\{I_{sd}^{-SMase} - I_{sd}^{+SMase} \times (I_{chol}^{-SMase}/I_{chol}^{+SMase})\}/I_{sd}^{-SMase}$, assuming that SM and DOPC give the same intensity. I_{chol}^{+SMase} and I_{chol}^{-SMase} were not affected by the SMase treatment, and were used as internal controls.

3. Results and discussion

3.1. Domain morphology in GUVs composed of DOPC/C_{16}Cer/C_{16}SM/cholesterol

We compared the structure of domains in GUVs that were prepared from 1:X:1–X:1 mixture of DOPC/C_{16}Cer/C_{16}SM/cholesterol, where X=0, 0.25 ,0.5, 0.6, 0.75, 1. The domains in GUVs were visualized at room temperature with TR-DPPE that has been shown to distribute mainly in the lipid phase with lower order [12,14,17]. Fig. 2A and B show two GUVs with different C_{16}Cer contents (X=0 and 0.25, respectively). In the

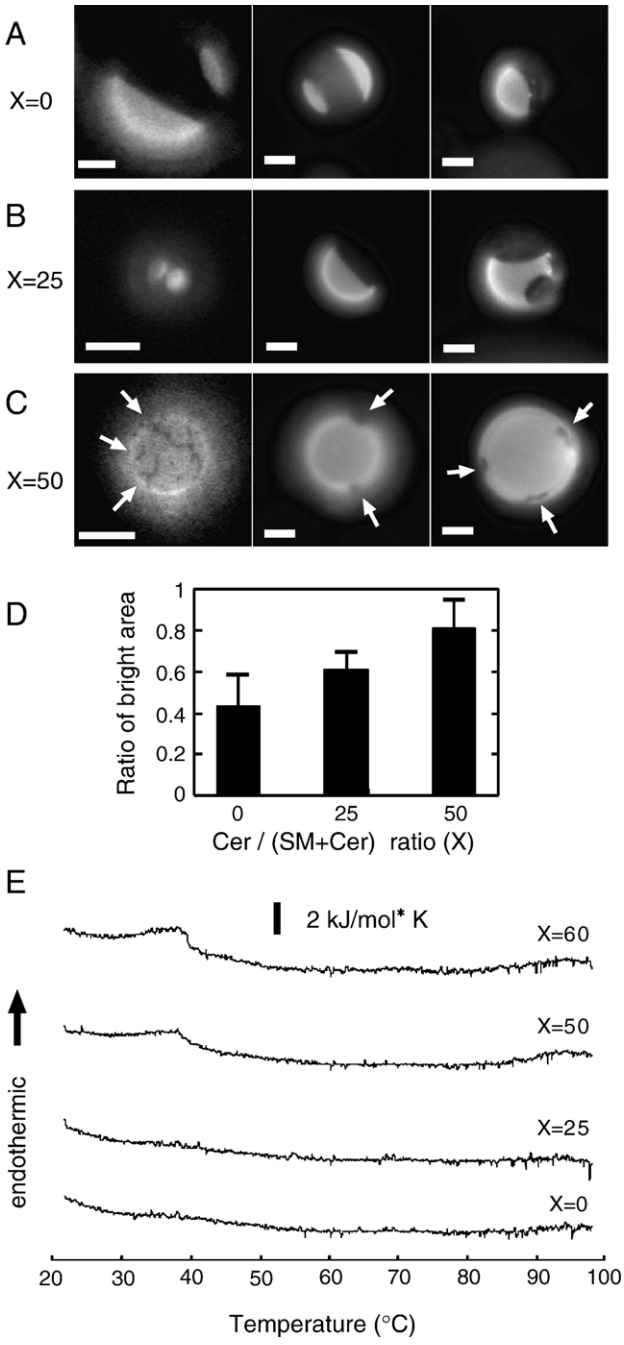

Fig. 2. Domain structure in GUVs containing various amount of Cer. GUVs were prepared from 1:X:1–X:1 mixture of DOPC/C_{16}Cer/C_{16}SM/cholesterol (molar ratio). (A) X=0; (B) X=0.25 (i.e., molar ratio of Cer was 8.3% of total lipid); (C) X=0.5 (17% of total lipid). The arrows indicated the irregular-shaped dark domain. Domains were visualized with TR-DPPE (0.1 mol% of total lipid). Observations were performed at room temperature (22–25 °C). Scale bars were 10 μm. (D) The ratio of projected area of the bright domain to the total GUV area. Values were the mean and S.D. of 15 vesicles. (E) DSC thermograms of MLVs. Lipid composition from the bottom to the top: X=0, 25, 50 and 60. The total lipid concentration was 3 mM. The heating rate was 0.5 K/min.

case of $X=0$ round, domains with bright fluorescence were apparent. We occasionally observed coalescence of two round domains indicating liquid nature of the round-shaped domains (see Fig. 3A). The round shape of these domains is an indication of coexistence of liquid-ordered and liquid-disordered phases, the latter of which was distributed with TR-DPPE [12,14,17]. The phase coexistence state was stable during observation (of the order of a few hours). A study of the phase diagram has also demonstrated the coexistence of liquid-ordered and disordered phases [50–52]. At $X=25$, similar round domains were formed (Fig. 2B left and middle), though the contrast of domains in some vesicles was inversed (Fig. 2B right). This indicated that the ratio of the projected area of bright domain was increased, which was clearly shown in Fig. 2D. Thus, liquid-ordered and liquid-disordered phases coexisted at low Cer contents. On the other hand, at $X=0.5$ structure and morphology of the domain was completely different (Fig. 2C): bright domains were larger and irregular-shaped, narrow dark domains appeared (arrows). The distribution of TR-DPPE suggests that at $X=0.5$ bright domains that occupied most of the membrane was in less ordered state and the dark domains were in more ordered state. Similar narrow domains with irregular border have been observed and explained as separation of ordered (gel) and liquid phases [11,44,53]. When $X\geq 0.75$, lipid aggregates, but no GUVs, were observed (not shown).

Fig. 2E shows results of differential scanning calorimetry (DSC) of MLVs composed of the same lipid mixture as above. Endothermic peak was absent below $X\leq 0.25$ indicating that the latent heat was negligibly small or null. The absence of the peak in thermogram has been reported for MLVs with similar lipid composition (1:1:1 mixture of DOPC/brain SM/cholesterol [54]). On the other hand, at $X\geq 0.5$, where elongated domains were observed in GUVs, an endothermic peak appeared at 37 °C, and the area of the peak was larger at $X=0.6$, suggesting that the transition enthalpy depended on Cer concentration in the membrane. C_{16}Cer has the phase transition temperature of 80 °C [55], the highest among the lipids contained in the GUVs. Cer is poorly miscible with phospholipids, possesses low affinity to cholesterol and tends to form a Cer-rich phase when Cer content is high [56]. We presume that the peak represented the melting of Cer-rich, gel or gel-like phase, and the dark domain that was observed in the GUVs with high Cer content was Cer-rich.

3.2. Disruption of liquid-ordered and liquid-disordered domain structure induced by enzymatic action of SMase

We then investigated the effect of the conversion of SM to Cer catalyzed by SMase on the structure of the domains in GUVs. SMase solution was applied to the external

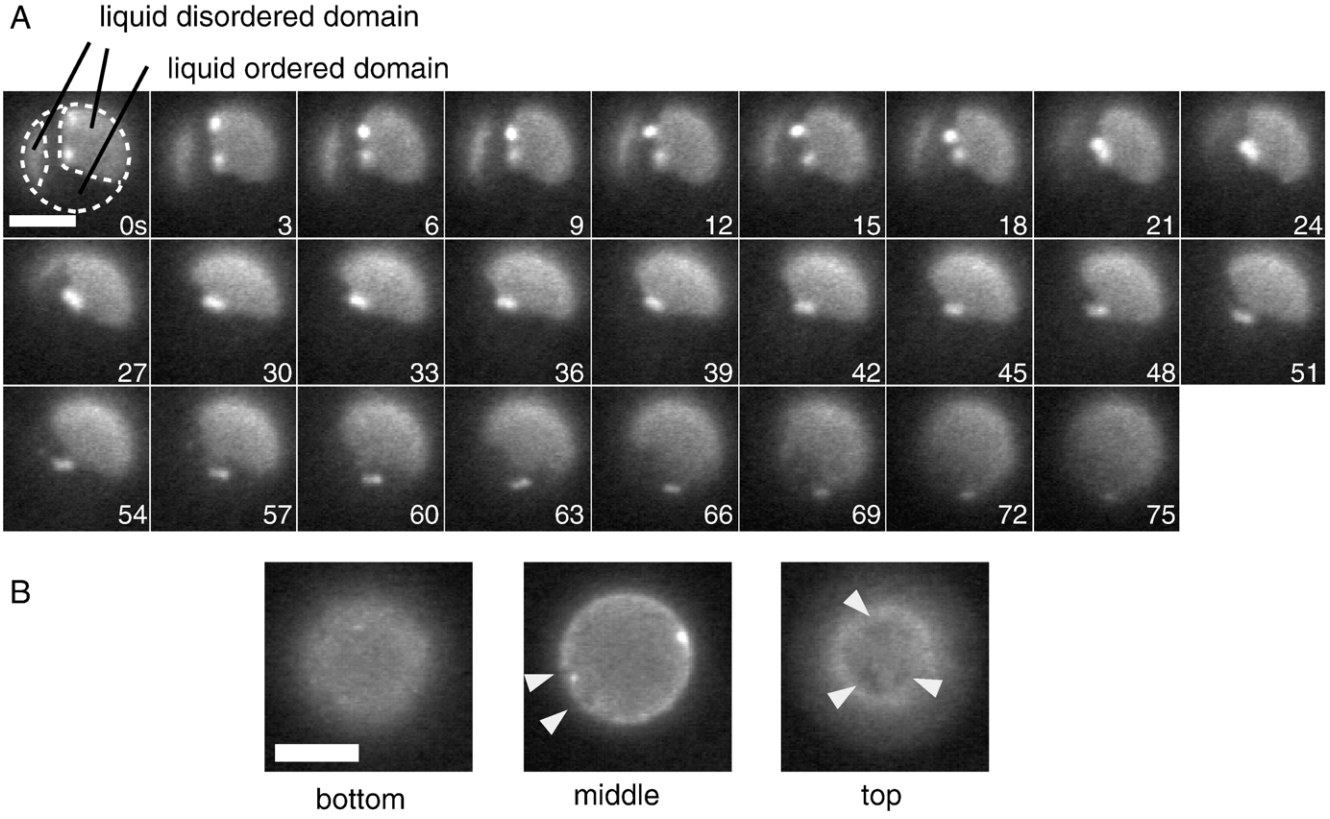

Fig. 3. (A) A sequence of images showing the process of SMase-induced alteration of domain structure. Numbers in each panel show the time (in s) elapsed from the start of the record. Until 27 s, two domains were apparent; during 27–33 s they fused to each other. Then, at 33 s domain boundary started undulating; it became noticeable at 39 s. At 57 s, TR-DPPE began to spread into the dark region. The dots were small vesicles attached on the larger vesicle. They showed Brownian movement (see Supplemental movie), which can represent surface movements. (B) Images of the same GUV as in panel A, but were acquired at three different focus levels 10 min after the addition of SMase. Initial composition of the GUV was DOPC/C_{16}SM/cholesterol = 1:1:1 (molar ratio) + 0.1 mol% TR-DPPE. Scale bars were 10 μm.

surface of GUVs composed of DOPC/C_{16}SM/cholesterol (1:1:1 mixture), which had been labeled with TR-DPPE, and the subsequent changes in the domain structure was observed at the video rate (30 frames/s). SMase treatment sometimes caused collapse of GUVs within a few minutes (13 out of 40 GUVs observed), before any change in the domains was observed. The collapse seemed to occur independently of the change in the domains, because GUVs containing no cholesterol also collapsed upon SMase treatment (Taniguchi et al., manuscript in preparation). It has been shown that SMase treatment of GUVs (SOPC/C_{16}SM=3:1) caused membrane invagination [24], but under our experimental conditions, it was not observed. The reason for the difference may be due to the difference in the method of GUV preparation: we adopted hydration method while the electro-formation method [57] was adopted in the previous study. The GUVs observed in the previous study were connected to lipid film on electrode, and hence change of surface tension can be compensated by movement of lipid molecules. On the other hand, the membranes of GUVs observed in this study seemed to be tensed because they sedimented on a cover glass (see Section 2.3) and their surface areas tended to decrease due to smaller molecular area of Cer (0.4 nm^2) than that of SM (0.7 nm^2) [58,59]. These differences could make the response of GUVs to physical perturbation quite differently, because local deformability of GUVs strongly depends on its membrane tension [60]. Thus, GUVs in our study were more difficult to change their shape. Previously, similar difference was found in the case of the studies of the activity of PLC on GUVs [61,62].

In GUVs that did not collapse, alteration of domain morphology was observed (n=27). In the GUVs shown in Fig. 3A, two circular domains existed until 27 s; during 27–30 s they fused to each other. Fusion was often seen without addition of SMase. However, subsequent phenomena were observed only in the presence of SMase: the undulation of domain edge became noticeable (39–57s, see supplemental movie), the area labeled by TR-DPPE broadened (57–75s), and finally, the labeled area spread over almost the entire surface of the GUV, which was apparent from the fluorescence images acquired at different focus levels after the change ceased (Fig. 3B). No such change was observed when the buffer alone (10 mM HEPES–NaOH, 0.1 mg/ml BSA, pH 7.4) was applied to GUVs (not shown). Fig. 3B shows that there are small regions with contrast darker than the surrounding areas (arrowheads) suggesting that lipid distribution was not uniform presumably due to the low miscibility of Cer with other lipids. We presume that the domain structure observed after the SMase treatment was similar to what was present in the GUVs prepared in the presence of high Cer/SM ratio.

Since GUVs are far larger than lipid molecules, one can assume that the lipid composition of the outer and the inner leaflet was initially the same, and domains existed in both leaflets. Perhaps, structures of the outer and the inner domains were the same, as previously suggested in similar lipid system [12]. If domains in the inner leaflet were not altered by SMase, the coexisting domains should be observed after the SMase treatment. Therefore, it was speculated that the SMase treatment resulted in alteration of the domains in both leaflets (see Section 3.4).

The degree of SM to Cer conversion under the microscopic experiment was difficult to estimate because of difficulty in controlling the amount of SMase applied on individual GUVs. In a separate experiment we compared the lipid composition of GUVs before and after the SMase treatment in the test tube by TLC. After incubation of GUVs containing 50 nmol C_{16}SM with 0.2 U SMase for 10 min at 25 °C, 36% of the C_{16}SM was converted into C_{16}Cer. The solution of GUVs contained significant amount of multilamellar giant vesicles, due to which the amount of total SM acted on by SMase was uncertain. Nevertheless, this result implies that the rate of conversion of SM to Cer was considerably high under the condition of observation and we claim that the dynamic and rapid change shown in Fig. 3 occurred as a result of the hydrolysis of SM.

3.3. Change in GP values of lipid membranes of GUVs accompanying conversion of SM to Cer

SMase-induced changes of the domain structure were also studied with Laurdan, an environment-sensitive dye. It has been shown that the regions with high and low-GP correspond to the liquid-ordered and liquid-disordered domains, respectively [12]. Fig. 4 shows a GUV labeled with Laurdan. Before addition of SMase (0 min), it was apparent that a large region with high-GP (blue: 0.65) (representing the liquid-ordered state) and a small region with low-GP (orange: 0.25) region (the liquid-disordered state) coexisted within the liposome. Corresponding to this, the distribution of GP values initially (0 min) possessed one sharp peak around 0.65 and another very broad one below 0.4 (downward arrow). In the presence of SMase the GP images of the GUV show that the boundary of the regions started disappearing 2 min after the SMase addition, became obscure during 3–4 min and finally disappeared (images in Fig. 4). This change was reflected in the distribution of GP values that exhibited the leftward shift of the higher peak of GP and rightward shift of the lower peak; finally, only one peak was detectable (the bottom trace). Similar observation was made with 14 other samples. No change in the distribution of GP values was observed when the buffer alone (HEPES-NaOH 10 mM, 10 mM, BSA 0.1 mg/ml, pH 7.4) was applied to GUVs.

Close inspection of the color panel in the right row in Fig. 4 indicates that small regions with higher GP values (hence in more highly ordered state; arrow) persisted for as long as 10 min after the addition of SMase. Although this was not apparent in the GP trace (bottom), presumably because the area of these regions was relatively small, the high-GP regions were consistently observed. The GP values indicate that these regions were in a state of higher order and were probably Cer-rich gel-like domains, which were observed after the SMase treatment (Fig. 3B).

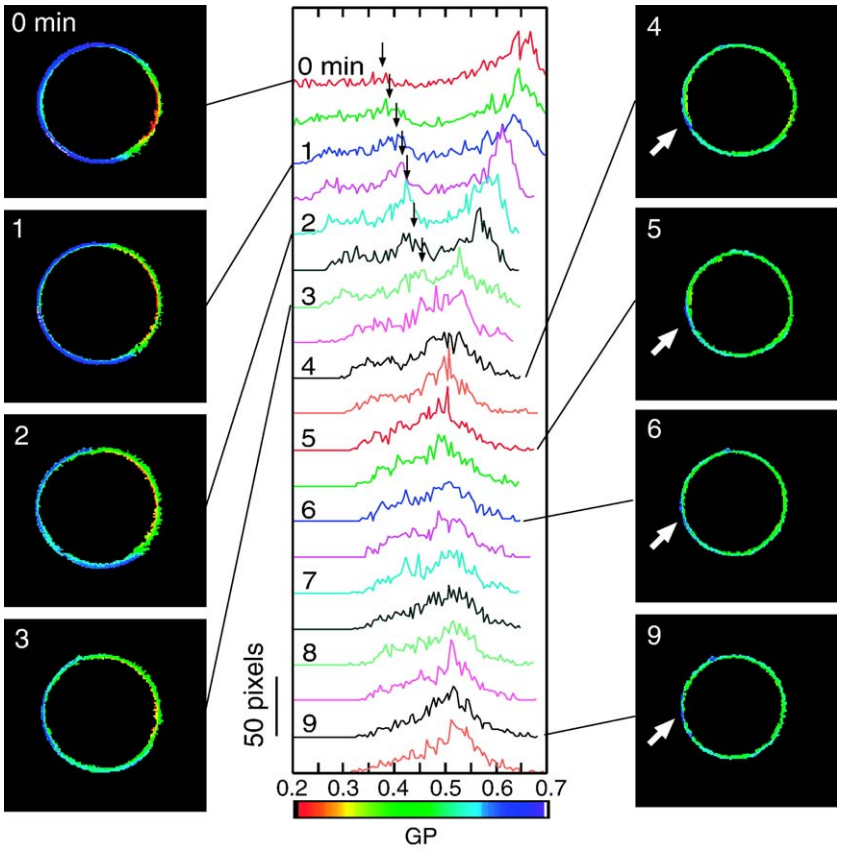

Fig. 4. Alteration of domain structure visualized with Laurdan. The color panels in right and left columns are GP-images calculated from the 440 nm and 490 nm images at indicated times. The middle column shows the change in the distribution of GP values of the contour of GUV. Initially, regions with high-GP value (blue) and those with low-GP value (red to green) coexisted. Four minutes after the addition of SMase, GP distribution became almost uniform, although smaller regions with higher GP values were present (arrow). Initial composition of the GUV was DOPC/C_{16}SM/cholesterol = 1:1:1 (molar ratio) + 1 mol% Laurdan. Scale bars were 10 μm.

3.4. Change in the structure of domains as a result of SM to Cer conversion

We have shown that the enzymatic conversion of C_{16}SM to C_{16}Cer induced global change in the pre-formed domain structure in GUVs: initially, the round-shaped, liquid-disordered domains were floating in dark domains. The conversion induced broadening of the round-shaped domains and resulted in coexistence of broad fluorescent domains with less fluorescent narrow domains. At higher Cer content a different type of domain structure appeared: it consisted of broad, fluorescent domains bordered by narrow, less fluorescent domains. The DSC measurement on the MLVs of the same compositions suggested that the less fluorescent domain was perhaps enriched with Cer. The image-based GP measurement of GUVs demonstrated that as a result of the enzymatic conversion, the initially existed regions with high and low order disappeared and a region with an intermediate order and small regions with the high order appeared. In the latter phase lipids may be enriched with Cer. The appearance of the highly-ordered phase was consistent with previous studies which have showed that Cer tends to form gel phase in DPPC [26,28], DMPC [29,30], POPC [22,26,27] and SM/cholesterol [26] membranes. At low contents of Cer, the ratio of liquid-ordered domain was decreased with increasing Cer, namely with decreasing SM (Fig. 2D). To our knowledge, SM and PC with saturated fatty acids are the only lipids which have the ability of formation of liquid-ordered phase. Close packing between the lipid and

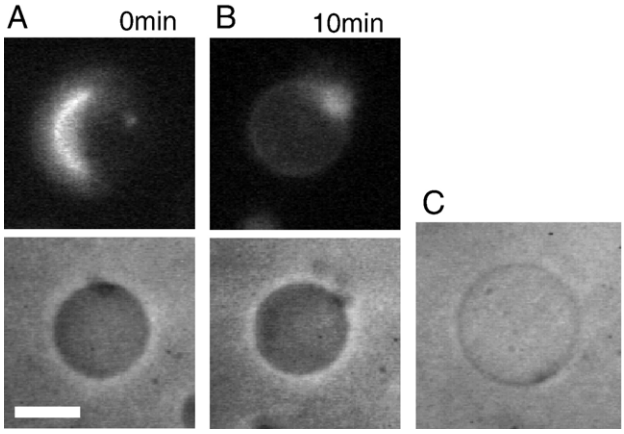

Fig. 5. (A and B) Fluorescence (upper) and corresponding phase-contrast (lower) images of a GUV acquired (A) 0 and (B) 10 min after the addition of SMase. The dark contrast of the GUV remained unchanged during the alteration of domain structure. (C), a phase-contrast image of another GUV placed in the medium containing sucrose instead of glucose demonstrates that the contrast of the inside of vesicle was the same as the outside. Initial lipid composition of the GUVs was DOPC/C_{16}SM/cholesterol = 1:1:1 (molar ratio) + TR-DPPE 0.1 mol %. Scale bars were 10 μm.

cholesterol molecules was an important factor to form liquid-ordered phase. Cer seemed to have lower ability to form the liquid-ordered phase because of its small polar headgroup. Moreover, Cer may compete against cholesterol for interaction with SM [34]. Therefore, the decrease of liquid-ordered phase was quite reasonable.

Previously, SMase-induced Cer-rich domain in PC or SM monolayer was visualized and dark rounded and dark branched domains were observed with increase of Cer content [31–33]. In this study, the effect of the conversion on pre-formed liquid-ordered and liquid-disordered domains in GUVs was visualized. The effect of hydrolysis of SM, which was reflected in the drastic change in the order of the lipids, seemed to occur in the inner as well as in the outer leaflet within a few minutes after the start of hydrolysis of SM. This is remarkable, because the size of SMase is too large to rapidly penetrate GUV membranes (for example, molecular weight of SMase from *Bacillus cereus* is 40 kDa). The mixing of the lipids between the outer and the inner leaflet by transbilayer diffusion (flip-flop) of lipids is also too slow to explain the result: previous measurements have shown the characteristic time of hours to days for phosphatidylcholine [63,64] and SM [65], and ~20 min for Cer [65]. There are some reports that Cer raises permeability of lipid membranes [66,67]. However, aqueous linking pore seems to be also unlikely; if this had occurred, sucrose (a content of GUVs) and glucose in the surrounding medium should have exchanged and the contrast of GUVs in phase contrast images should have been lost. Indeed, it was not the case as shown in Fig. 5, which compares fluorescence and phase contrast images of the same GUV before and after the SMase treatment. The bright domain visualized with TR-DPPE before the SMase treatment (upper panel of Fig. 5A) disappeared 10 min after the SMase treatment (Fig. 5B, upper panel), but the dark contrast of the GUV remained unchanged (lower panels). The GUV shown in Fig. 5C was placed in a medium containing sucrose instead of glucose so that its contrast was equal to that of the surrounding medium. Comparison of three phase contrast images indicates that there was no measurable loss of contrast during the SMase action, and the possibility of the formation of linking pores is remote. Another possibility is that SMase and Cer promote transbilayer movement of lipid, which was shown by fluorescence-based studies on LUVs recently [68,69]. This is attributable to the ability of Cer to cause lamellar to non-lamellar phase transition in lipid bilayer [70]. The facilitation of transbilayer movement of lipids is likely to occur in GUVs and might cause alteration of domains in the inner leaflet.

3.5. Biological relevance

It has been established that several biological signals enhance SMase activity, thereby reducing the cellular level of SM and raising the level of Cer. The kinetics of Cer production in vivo is complex [71]. Approximately 30 to 40% reduction in the total amount of cellular SM and 3 to 5 fold increase of that of Cer occur within 10 min after binding of tumor necrosis factor-α or infection of bacteria and virus [72–76]. The above figures of the conversion may be underestimated, because the conversion occurs in plasma membrane [73,77] (the content of SM in plasma membrane is typically 15–20% [78]) and SM in other cellular organelles is probably unaffected. Therefore, based on our observation and other reports, we speculate that in vivo the SM to Cer conversion can rapidly alter the assembly of lipid microdomains thereby kinetically affecting the process of signal transduction (modulation of kinetic parameters, on–off switching, etc.). Interestingly, SMase treatment of the cell induces clustering of some membrane proteins during apoptosis [75,76,79]. A role of SMase in this case seemed to be modulation of assembly of lipid microdomains.

Acknowledgments

This work was supported by Grant-in-Aid for COE Research and Grant 14658208 from The Ministry of Education, Culture, Sports, Science and Technology, Japan and Ground Research for Space Utilization promoted by NASDA and Japan Space Forum. We thank Dr. Ken-ichirou Akashi for his technical advises in the early stage of this work.

Appendix A. Supplementary data

Supplementary data associated with this article can be found in the online version at doi:10.1016/j.bbamem.2006.02.026.

References

[1] K. Simons, E. Ikonen, Functional rafts in cell membranes, Nature 387 (1997) 569–572.
[2] L.J. Foster, C.L. de Hoog, M. Mann, Unbiased quantitative proteomics of lipid rafts reveals high specificity for signaling factors, Proc. Natl. Acad. Sci. U. S. A. 100 (2003) 5813–5818.
[3] G. Vereb, J. Szöllosi, J. Matkó, P. Nagy, T. Farkas, L. Vigh, L. Mátyus, T.A. Waldmann, Dynamic, yet structured: the cell membrane three decades after the Singer–Nicolson model, Proc. Natl. Acad. Sci. U. S. A. 100 (2003) 8053–8058.
[4] M. Edidin, Shrinking patches and slippery rafts: scales of domains in the plasma membrane, Trends Cell Biol. 11 (2001) 492–496.
[5] S.L. Regen, Lipid–lipid recognition in fluid bilayers: solving the cholesterol mystery, Curr. Opin. Chem. Biol. 6 (2002) 729–735.
[6] S. Munro, Lipid rafts: elusive or illusive? Cell 115 (2003) 377–388.
[7] T. Yokoyama, J. Du, Y. Kawamoto, H. Suzuki, Inhibition of Fas-mediated apoptotic cell death of murine T lymphocytes in a mouse model of immunosenscence in linkage to deterioration in cell membrane raft function, Immunology 112 (2004) 64–71.
[8] B.S. Wilson, S.L. Steinberg, K. Liederman, J.R. Pfeiffer, Z. Surviladze, J. Zhang, L.E. Samelson, L. Yang, P.G. Kotula, J.M. Oliver, Markers for detergent-resistant lipid rafts occupy distinct and dynamic domains in native membranes, Mol. Biol. Cell 15 (2004) 2580–2592.
[9] M. Heffer-Lauc, G. Lauc, L. Nimrichter, S.E. Fromholt, R.L. Schnaar, Membrane redistribution of gangliosides and glycosylphosphatidylinositol-anchored proteins in brain tissue sections under conditions of lipid raft isolation, Biochim. Biophys. Acta 1686 (2005) 200–208.
[10] D. Lichtenberg, F.M. Goñi, H. Heerklotz, Detergent-resistant membranes should not be identified with membrane rafts, Trends Biochem. Sci. 30 (2005) 430–436.

[11] G.W. Feigenson, J.T. Buboltz, Ternary phase diagram of dipalmitoyl-PC/dilauroyl-PC/cholesterol: nanoscopic domain formation driven by cholesterol, Biophys. J. 80 (2001) 2775–2788.
[12] C. Dietrich, L.A. Bagatolli, Z.N. Volovyk, N.L. Thompson, M. Levi, K. Jacobson, E. Gratton, Lipid rafts reconstituted in model membrane, Biophys. J. 80 (2001) 1417–1428.
[13] A.V. Samsonov, I. Mihalyov, F.S. Cohen, Characterization of cholesterol–sphingomyelin domains and their dynamics in bilayer membranes, Biophys. J. 81 (2001) 1486–1500.
[14] S.L. Veatch, S.L. Keller, Organization in lipid membranes containing cholesterol, Phys. Rev. Lett. 89 (2002) 268101.
[15] T. Baumgart, S.T. Hess, W.W. Webb, Imaging coexisting fluid domains in biomembrane models coupling curvature and line tension, Nature 425 (2003) 821–824.
[16] D. Scherfeld, N. Kahya, P. Schwille, Lipid dynamics and domain formation in model membranes composed of ternary mixtures of unsaturated and saturated phosphatidylcholines and cholesterol, Biophys. J. 85 (2003) 3758–3768.
[17] S.L. Veatch, S.L. Keller, Separation of liquid phases in giant vesicles of ternary mixtures of phospholipids and cholesterol, Biophys. J. 85 (2003) 3074–3083.
[18] C. Dietrich, B. Yang, T. Fujiwara, A. Kusumi, K. Jacobson, Relationship of lipid rafts to transient confinement zones detected by single particle tracking, Biophys. J. 82 (2002) 274–284.
[19] D.H. Nguyen, D.D. Taub, Inhibition of chemoline receptor function by membrane cholesterol oxidation, Exp. Cell Res. 291 (2003) 36–45.
[20] K. Gaus, E. Gratton, E.P.W. Kable, A.S. Jones, I. Gelissen, L. Kritharides, W. Jessup, Visualizing lipid structure and raft domains in living cells with two-photon microscopy, Proc. Natl. Acad. Sci. U. S. A. 100 (2003) 15554–15559.
[21] E. Gulbins, R. Kolesnick, Raft ceramide in molecular medicine, Oncogene 22 (2003) 7070–7077.
[22] J.M. Holopainen, M. Subramanian, P.K.J. Kinunnen, Sphingomyelinase induces lipid microdomain formation in a fluid phosphatidylcholine/sphingomyelin membrane, Biochemistry 37 (1998) 17562–17570.
[23] H.-W. Huang, E.M. Goldberg, R. Zidovertzki, Ceramides modulate protein kinase C activity and perturb the structure of phosphatidylcholine/phosphatidylserine bilayers, Biophys. J. 77 (1999) 1489–1497.
[24] J.M. Holopainen, M.I. Angelova, P.K.J. Kinunnen, Vectorial budding of vesicles by asymmetrical enzymatic formation of ceramide in giant liposomes, Biophys. J. 78 (2000) 830–838.
[25] X. Xu, R. Bittman, G. Duportail, D. Heissler, C. Vilcheze, E. London, Effect of structure of natural sterols and sphingolipids on the formation of ordered sphingolipid/sterol domains (rafts), J. Biol. Chem. 276 (2001) 33540–33546.
[26] J.B. Massey, Interaction of ceramides with phosphatidylcholine, sphingomyelin and sphingomyelin/cholesterol bilayers, Biochim. Biophys. Acta 1510 (2001) 167–184.
[27] Y.-W. Hsueh, Y.-W.R. Giles, N. Kitson, J. Thewalt, The effect of ceramide on phosphatidylcholine membranes: a deuterium NMR study, Biophys. J. 82 (2002) 3089–3095.
[28] D.C. Carrier, B. Maggio, Phase behavior and molecular interactions in mixtures of ceramide with dipalmitoylphosphatidylcholine, J. Lipid Res. 40 (1999) 1978–1989.
[29] J.M. Holopainen, J. Lemmich, F. Richer, O.G. Mouritsen, G. Rapp, P.K.J. Kinnunen, Dimyristoylphosphatidylcholine/C16:0-ceramide binary liposomes studied by differential scanning calorimetry and wide- and small-angle X-ray scattering, Biophys. J. 78 (2000) 2459–2469.
[30] J.M. Holopainen, H.L. Brockman, R.E. Brown, P.K.J. Kinnunen, Interfacial Interactions of ceramide with dimyristoylphosphatidylcholine: impact of the n-acyl chain, Biophys. J. 80 (2001) 765–775.
[31] J.P. Slotte, Lateral domain formation in mixed monolayers containing cholesterol and dipalmitoylphosphatidylcholine or N-palmitoylsphingomyelin, Biochim. Biophys. Acta 1235 (1995) 419–427.
[32] M.L. Fanani, S. Härtel, R.G. Oliveira, B. Maggio, Bidirectional control of sphingomyelinase activity and surface topography in lipid monolayers, Biophys. J. 83 (2002) 3416–3424.
[33] S. Härtel, M.L. Fanani, B. Maggio, Shape transitions and lattice structuring of ceramide-enriched domains generated by sphingomyelinase in lipid monolayers, Biophys. J. 88 (2005) 287–304.
[34] Megha, E. London, Ceramide selectively displaces cholesterol from ordered lipid domains (rafts), J. Biol. Chem. 279 (2004) 9997–10004.
[35] M. Koval, R.E. Pagano, Intracellular transport and metabolism of Sphingomyelin, Biochim. Biophys. Acta 1082 (1991) 113–125.
[36] T. Parasassi, G.D. Stasio, D. Ravagnan, R.M. Rusch, E. Gratton, Quantitation of lipid phases in phospholipid vesicles by the generalized polarization of Laurdan fluorescence, Biophys. J. 60 (1991) 179–189.
[37] T. Parasassi, E. Gratton, W.M. Yu, P. Wilson, M. Levi, Two-photon fluorescence microscopy of Laurdan generalized polarization domains in model and natural membranes, Biophys. J. 72 (1997) 2413–2429.
[38] T. Ohba, S. Tsuchiya, T. Kumeta, K. Ohki, Microscopic imaging of phase separation in a giant liposome by Laurdan at video rate, Jpn. J. Appl. Phys. 44 (2005) , 8733–8738.
[39] S. Gatt, T. Dinur, Y. Barenholz, A spectrophotometric method for determination of sphingomyelinase, Biochem. Biophys. Acta 530 (1978) 503–507.
[40] K. Akashi, H. Miyata, H. Itoh, K. Kinosita Jr., Preparation of giant liposomes in physiological conditions and their characterization under an optical microscope, Biophys. J. 71 (1996) 3242–3250.
[41] K. Akashi, H. Miyata, H. Itoh, K. Kinosita Jr., Formation of giant liposomes promoted by divalent cations: critical role of electrostatic repulsion, Biophys. J. 74 (1998) 2973–2982.
[42] K.A. Riske, H.-G. Döbereiner, Diacylglycerol-rich domain formation in giant stearoyl-oleoyl phosphatidylcholine vesicles driven by phospholipase C activity, Biophys. J. 85 (2003) 2351–2362.
[43] C.E. Bunker, T.L. Bowen, Y.-P. Sun, A photophysical study of solvatochromic probe 6-propionyl-2-(*N*,*N*-dimethylamino)naphthalene (prodan) in solution, Photochem. Photobiol. 58 (1993) 499–505.
[44] L.A. Bagatolli, E. Gratton, Two photon fluorescence microscopy of coexisting lipid domains in giant unilamellar vesicles of binary phospholipid mixtures, Biophys. J. 78 (2000) 290–305.
[45] K. Kinosita Jr., H. Itoh, S. Ishiwata, K. Hirano, T. Nishizawa, T. Hayakawa, Dual-view microscopy with a single camera: real-time imaging of molecular orientations and calcium, J. Cell Biol. 115 (1991) 67–73.
[46] Z. Mamdouh, M.C. Giocondi, C. Le Grimellec, In situ determination of intracellular membrane physical state heterogeneity in renal epithelial cells using fluorescence ratio microscopy, Eur. Biophys. J. 27 (1998) 341–351.
[47] K. Ohki, Formation of micro-domains as functional regions in biomembranes: specific interactions inferred by differential scanning calorimetry and microscopic imaging of membrane fluidity, J. Phys. Condens. Matter 17 (2005) 1–7.
[48] K. Ohki, K. Takahashi, S. Kato, A. Maesono, Short- and long-range Ca 2+-induced lateral phase separation in a ternary mixture of phosphatidic acid, phosphatidylcholine and phosphatidylethanolamine, Chem. Phys. Lipids 50 (1989) 109–117.
[49] T.A. Nurminen, J.M. Holopainen, H. Zhao, P.K.J. Kinnunen, Observation of topical catalysis by sphingomyelinase coupled to microspheres, J. Am. Chem. Soc. 124 (2001) 12129–12134.
[50] R.F.M. de Almeida, A. Fedorov, M. Prieto, Sphingomyelin/phosphatidylcholine/cholesterol phase diagram: boundaries and composition of lipid rafts, Biophys. J. 85 (2003) 2406–2416.
[51] R.F.M. de Almeida, L.M.S. Loura, A. Fedorov, M. Prieto, Lipid rafts have different sizes depending on membrane composition: a time-resolved fluorescence resonance energy transfer study, J. Mol. Biol. 346 (2005) 1109–1120.
[52] S.L. Veatch, S.L. Keller, Miscibility phase diagrams of giant vesicles containing sphingomyelin, Phys. Rev. Lett. 94 (2005) 148101.
[53] J. Korlach, P. Schwille, W.W. Webb, G.W. Feigenson, Characterization of lipid bilayer phase by confocal microscopy and fluorescence correlation spectroscopy, Proc. Natl. Acad. Sci. U. S. A. 96 (1999) 8461–8466.
[54] M. Gandhavadi, D. Allende, A. Vidal, S.A. Simon, T.J. McIntosh, Structure, composition, and peptide binding properties of detergent soluble bilayers and detergent resistant rafts, Biophys. J. 82 (2002) 1469–1482.
[55] J. Shah, J.M. Atienta Jr., R.I. Duclos, A.V. Rawlings, Z. Dong, G.G. Shipley, Structural and thermotropic properties of synthetic C16:0

(palmitoyl) ceramide: effect of hydration, J. Lipid Res. 36 (1995) 1936–1944.
[56] M.P. Veiga, J.L.R. Arrondo, F.M. Goñi, A. Alonso, Ceramides in phospholipid membranes: effects on bilayer stability and transition to nonlamellar phases, Biophys. J. 76 (1999) 342–350.
[57] M.I. Angelova, D.S. Dimitrov, Liposome electroformation, Faraday Discuss. Chem. Soc. 81 (1986) 303–311.
[58] H. Löfgren, I. Pascher, Molecular arrangements of sphingolipids. The monolayer behaviour of ceramides, Chem. Phys. Lipids 20 (1977) 273–284.
[59] M. Jungner, H. Ohvo, J.P. Slotte, Interfacial regulation of bacterial sphingomyelinase activity, Biochim. Biophys. Acta 1344 (1997) 230–240.
[60] W. Helfrich, R.M. Servuss, Undulations, steric interaction and cohesion of fluid membranes, Il Nuovo Cimento 3D (1984) 137–151.
[61] J.M. Holopainen, M.I. Angelova, T. Söderlund, P.K.J. Kinnunen, Macroscopic consequences of the action of phospholipase C on giant unilamellar liposomes, Biophys. J. 83 (2002) 932–943.
[62] K.A. Riske, H.-G. Döbereiner, Diacylglycerol-rich domain formation in giant stearoyl-oleoyl phosphatidylcholine vesicles driven by phospholipase C activity, Biophys. J. 85 (2003) 2351–2362.
[63] R. Homan, H.J. Pownall, Transbilayer diffusion of phospholipids: dependence on headgroup structure and acyl chain length, Biochim. Biophys. Acta 938 (1988) 155–166.
[64] W.C. Wimley, T.E. Thompson, Exchange and flip-flop of dimyristoylphosphatidylcholine in liquid-crystalline, gel and two-component, two-phase large unilamellar vesicles, Biochemistry 29 (1990) 1296–1303.
[65] J. Bai, R.E. Pagano, Measurement of spontaneous transfer and transbilayer movement of BODIPY-labeled lipids in lipid vesicles, Biochemistry 36 (1997) 8840–8848.
[66] L.R. Montes, M.B. Ruiz-Argüello, F.M. Goñi, A. Alonso, Membrane restructuring via ceramide results in enhanced solute efflux, J. Biol. Chem. 277 (2002) 11788–11794.
[67] L.J. Siskind, M. Colombini, The lipids C2- and C16-ceramide form large stable channels, J. Biol. Chem. 275 (2000) 38640–38644.
[68] F.X. Contreras, A.-V. Villar, A. Alonso, R.N. Kolesnick, F.M. Goñi, Sphingomyelinase activity causes transbilayer lipid translocation in model and cell membranes, J. Biol. Chem. 278 (2003) 37169–37174.
[69] F.-X. Contreras, G. Basañez, A. Alonso, A. Herrmann, F.M. Goñi, Asymmetric addition of ceramides but not dihydroceramides promotes transbilayer (flip-flop) lipid motion in membranes, Biophys. J. 88 (2005) 348–359.
[70] R.M. Raphael, R.E. Waugh, S. Svetina, B. ekš, Fractional occurrence of defects in membranes and mechanically driven interleaflet phospholipid transport, Phys. Rev., E 64 (2001) 051913.
[71] Y.A. Hannun, Functions of ceramide in coordinating cellular responses to stress, Science 274 (1996) 1855–1859.
[72] S. Chatterjee, Neutral sphingomyelinase action stimulates signal transduction of tumour necrosis factor-α in the synthesis of cholesteryl esters in human fibroblasts, J. Biol. Chem. 269 (1994) 879–882.
[73] P. Liu, R.G.W. Anderson, Compartmentalized production of ceramide at the cell surface, J. Biol. Chem. 270 (1995) 27179–27185.
[74] H. Grassmé, E. Gulbins, B. Brenner, K. Ferlinz, K. Sandhoff, K. Harzer, F. Lang, T.F. Mayer, Acidic sphingomyelinase mediates entry of *N. gonorrhoeae* into nonphagocytic cells, Cell 91 (1997) 605–615.
[75] H. Grassmé, V. Jendrossek, A. Riehle, G. von Kürthy, J. Berger, H. Schwarz, M. Weller, R. Kolesnick, E. Gulbins, Host defense against *Pseudomonas aeruginosa* requires ceramide-rich membrane rafts, Nat. Med. 9 (2003) 322–330.
[76] H. Grassmé, A. Cremesti, R. Kolesnick, E. Gulbins, Ceramide-mediated clustering is required for CD95-DISC formation, Oncogene 22 (2003) 5457–5470.
[77] A.E. Cremesti, F.M. Goni, R. Kolesnick, Role of sphingomyelinase and ceramide in modulating rafts: do biophysical properties determine biologic outcome? FEBS Lett. 531 (2002) 47–53.
[78] B. Alberts, A. Johnson, J. Lewis, M. Raff, K. Roberts, P. Walter, The Molecular Biology of the Cell, 4th ed., Garland Science, New York, 2002, p. 589.
[79] J. Kilkus, R. Goswami, F.D. Testai, G. Dawson, Ceramide in raft (detergent-insoluble fraction) mediates cell death in neurotumor cell lines, J. Neurosci. Res. 72 (2003) 65–75.